etadata, citation and similar papers at core.ac.uk
brought to you by
provided by Purdu

Low-Power Flexible Organic Light-Emitting Diode Display Device

Sunkook Kim, Hyuk-Jun Kwon, Sunghun Lee, Hongshik Shim, Youngtea Chun, Woong Choi, Jinho Kwack, Dongwon Han, MyoungSeop Song, Sungchul Kim, Saeed Mohammadi, InSeo Kee,* and Sang Yoon Lee**

Demands in extending flat panel approaches to attain ultra-thin flexible displays, which are lightweight, portable, and unbreakable for head-up displays, security identification documents, conformable products, and electronic papers are ever increasing.[1–3] A typical flexible display comprises two major parts: i) driving circuitry to switch and address the display device, and ii) a flexible display device to display an image and enhance outdoor readability. Significant progress has been made in achieving stable rollable or bendable driving circuitry based on flexible thin film transistors (TFTs), such as oxide transistors based on gallium indium zinc oxide (GIZO)[4] or hafnium indium zinc oxide (HIZO),[5] low temperature poly-Si (LTPS) on a plastic substrate (polyimide),[6] nanotube and nanowire-based transistors,[2,7,8] and organic thin film transistors (OTFTs).[9] On the other hand, challenges to integrate a flexible display device to realize full-color, low power, and outdoor readability have still not been addressed. Liquid crystal displays (LCDs) are widely used to fabricate commercial displays, but their optical system to switch a light source (backlight unit or light-emitting diode (LED) through a red/green/blue (RGB) color filter) consists of a constant thick layer of liquid crystal molecules aligned between electrodes, and two polarization films having the axes of transmission perpendicular to each other. Bending a LCD causes liquid crystal molecules to deform. The light that passes through the deformed liquid crystal molecules and two surrounding polarizing films with perpendicular polarization axes is distorted causing display malfunction. In comparison, OLEDs do not suffer from such bending malfunctions, which makes OLEDs strong candidates for integration with flexible electronics to achieve flexible color displays.

S. Kim, H.-J. Kwon, H. Shim, Y. Chun, W. Choi, Prof. I. S. Kee, Prof. S. Y. Lee
Samsung Advanced Institute of Technology
San # 14-1 Nongseo-do
Giheung-gu, Yongin-si, Gyeonggi-do, 446-712, Korea
E-mail: kimskcnt@gmail.com; is.kee@samsung.com; sangyoon.lee@samsung.com
Prof. S. Mohammadi
School of Electrical and Computer Engineering and Birck Nanotechnology Center
Purdue University
West Lafayette, IN 47907, USA
S. Lee, J. Kwack, D. Han, M.-S. Song, S. Kim
Samsung Mobile display
San # 14-1 Nongseo-dong, Yongin-si, Geyonggi-do, 446-71,1 Korea

DOI: 10.1002/adma.201101066

Current-generation OLEDs can afford a high performance and flexibility, but this technology requires a polarization (POL) film to enhance the contrast ratio for outdoor readability, and glass encapsulation to protect the OLED from oxygen and water. The fragile nature of these components limits their utility in flexible OLED display devices. An advanced material to overcome the fragile components is required to allow the flexible properties. In order to achieve a highly flexible OLED display device, the following characteristics are needed: i) a low temperature process to prevent deformation in plastic substrates, ii) a new optical architecture providing both flexibility and high outdoor readability, iii) a thinner and lighter platform than for current OLED technologies that allows bending and folding, iv) mechanical and electrical stability during repetitive folding, and v) optical reliability without malfunction from an ambient environment, especially water and oxygen.

In this paper, we report for the first time a flexible OLED display device having a top emission structure composed of an OLED microcavity covered with thin film encapsulation (TFE) and a low temperature color filter (LTCF). Here, LTCFs and a microcavity are utilized to reduce reflected light thus enhance outdoor readability, where the primary wavelength is filtered by the LTCFs with a transmission factor of 70–95%, and the destructive interferences of the OLED microcavity reduce the overall reflectance to below 50%. Through the novel optical architecture, contrast ratios of 14:1 at 500 lux and 150 000:1 in dark ambient are achieved. Interestingly, the new optical system can lower the power consumption of the OLED panel by as much as 30%, compared to current OLED technology that utilizes POL films. Furthermore, the realized flexible OLED device which employs LTCFs (a photosensitive resist including cross-linking monomer and diacrylate) and TFE (multi-pairs of Al_2O_3 and polyacrylate),[10] which are specifically designed at low temperature processes under 90 °C, is compatible with conventional OLED technology (OLEDs can be easily damaged above 100 °C). The TFE can provide the OLED long-term reliability to block oxygen and ambient water. The prototype OLED display device (OLED, LTCF, and TFE) exhibits an overall thickness of 8 μm, the thinnest among commercially available display devices. The development of these techniques can afford a highly flexible OLED display with low power consumption and high outdoor readability.

Figure 1 shows a proof-of-concept of a flexible display device with a LTCF and TFE placed on a RGB OLED microcavity. The processing starts with patterning OLED devices onto plastic substrates. RGB OLED pixel devices are formed. These

© 2011 WILEY-VCH Verlag GmbH & Co. KGaA, Weinheim

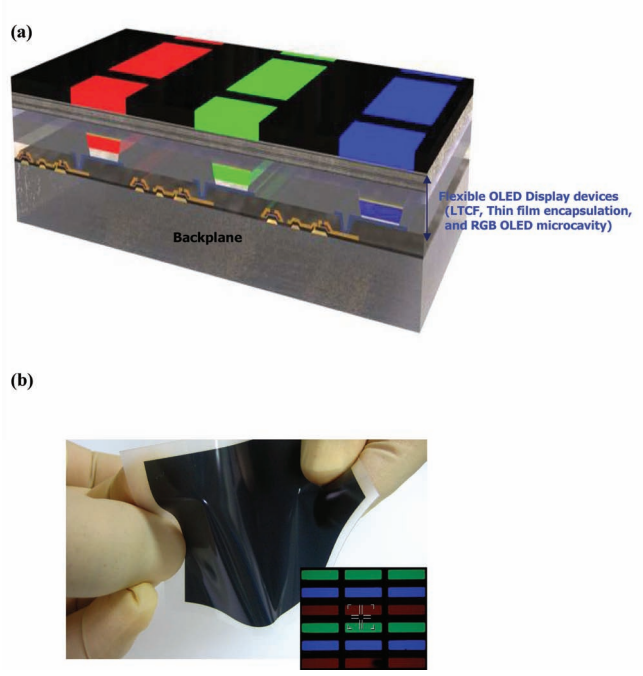

Figure 1. a) Cross-section diagram of the proposed flexible OLED display device composed of a LTCF, TFE, and a RGB OLED microcavity. The standard RGB pixel device has glass/Ag (200 nm)/ITO (10 nm)/HIL (60 nm)/HTL/EML (30 nm)/ETL (30 nm)/Mg:Ag (10:1, 15 nm)/CPL (60 nm)/TFE layers. b) Photograph of flexible OLED display device (LTCF, TFE, and RGB OLED microcavity) on plastic substrate, showing the mechanical flexibility. (inset) Real optical image of the RGB/BM color filter. All layers are patterned by standard photolithography below 90 °C

devices consist of i) a bi-layer Ag (200 nm)/indium tin oxide (ITO) (10 nm) anode, ii) an OLED device with multiple layers of a hole-injection layer (HIL)/hole-transport layer (HTL)/emissive layer (EML)/electron transport layer (ETL) OLED layer, iii) a bi-layer of Mg:Ag (10:1, 15 nm) cathode, and iv) an organic capping layer (CPL). The thickness of the HTL material is varied for different color wavelengths, where the thickness of the HTL is 60, 120, 175 nm for blue, green, and red, respectively. The multilayer OLED devices consist of i) HIL: 2T-NATA (4,4′,4″-tris(*N*-(naphthalen-2-yl)-*N*-phenylamino)-triphenylamine), ii) HTL: NPB (*N*,*N*′-bis(naphthalen-1-yl)-*N*,*N* ′-bis(phenyl)benzidine), iii) Blue-EML (5 wt% doping): MADN (2-methyl-9,10-di(2-napthyl)anthracene) (blue host), DSA-Ph (1,4-di-[4-(*N*,*N* -diphenyl)amino]styrylbenzene) (blue dopant), Green-EML (5 wt% doping): MADN (green host): C545T (2,3,6,7-tetrahydro-1,1,7,7,-tetramethyl-1*H*,5*H*,11*H*-10-(2-benzothiazolyl)quinolizino[9,9a,1gh]coumarin), Red-EML (10 wt% doping): BAlq (bis(2-methyl-8-quinolinolato)(*para*-phenylphenolato) aluminium(III)) (red host), Ir(piq)2(acac) (bis(1-phenylisoquinoline)(acetylacetonate)iridium(III)) (red dopant), iv) ETL: Alq3 (tris(8-hydroxy-quinolinato)aluminium), and v) CPL:NPB. Different hosts/dopants in RGB EML layers can emit different colors when an electric current passes through the OLED device. The thick Ag (200 nm) anode reflects the light generated in the EML materials, while a semi-transparent thin Mg/Ag cathode is employed to obtain electromagnetic radiation from the cavity. CPL is used to enhance the light out-coupling efficiency. The deposition of the organic and metal layers are carried out by thermal evaporation under vacuum (10^{-7} torr) with separate deposition chambers for organic transport layers, light emitting layers, and metal contacts. However, organic electroluminescent (EL) materials are easily oxidized by water and oxygen. In order to prevent oxidization, flexible OLED devices are encapsulated with a multilayered thin-film oxide layer (200–500 nm thick Al_2O_3 deposited by reactive sputtering process at 80 °C) as a barrier layer and a thin-film polymer layer (0.25 to 4 μm of Barix (proposed by Vitex)) as a planarization layer.[10] The polymer layers, a mixture of photosensitive acrylate monomers, are vaporized under vacuum followed by UV curing to facilitate polymerization. Finally, a standard photolithography is performed to pattern RGB color filters and black matrix (BM) on the OLED panel in a regular sequence.

In the presence of outdoor light, the contrast ratio of the luminance of the brightest color (white) to that of the darkest color (black) may be lowered by reflecting anode and cathode metal electrodes in the OLED microcavity. In standard displays, POL films are employed to increase the contrast ratio and thus improve the outdoor readability. Conventional POL films consist of microscopic herapathite crystals, which are made from poly(vinyl alcohol) (PVA) plastic with iodine doping.[11] Stretching of the sheet during manufacture ensures that the PVA chains are aligned in one particular direction, where the polarized light parallel to the chains is absorbed by the sheet. On the other hand, PVA chains are not flexible and can be easily broken along the polarization direction.

To achieve a flexible OLED display with high outdoor readability, a combination of an OLED microcavity and color filter is designed and employed to minimize the reflectance of the OLED panels without a need for brittle POL films (see **Figure 2**a). The primary wavelength that passes through the color filter is subsequently subjected to a destructive interference by the OLED microcavity where waves r_1 (the reflected light from cathode) and r_2 (the reflected light from anode) in Figure 2 a end up exactly out of phase. The OLED microcavity formed by a highly reflective anode mirror (thick Ag/ITO) and a semi-transparent cathode mirror (thin Mg/Ag) are designed with a specific thickness (L) in order to achieve a standing wave inside the microcavity. By varying the thickness of the HTL of the OLED while keeping the remaining thicknesses of the HIL, EML, and ETL constant, OLED layer thicknesses of 180, 240, and 295 nm for red, green, and blue are achieved, respectively. To undergo fully destructive interference between lights reflected from the anode (r_2) and the semi-transparent cathode (r_1), the total optical thickness L is set at

$$L = \sum_j (n_{j\lambda} d_j) = \frac{\lambda_0}{4\pi}(2\pi \cdot q + \delta_a + \delta_c) \quad (1)$$

where λ_0 is the resonance wavelength in air, q is a zero or positive integer, $n_{j\lambda}$ and d_j are the dispersive refractive index and physical thickness of the j^{th} layer in the OLED, respectively, and δ_a and δ_c are the phase shift at the anode and cathode (blue: $\delta_a \sim 1.38\Pi$, $\delta_c \sim 1.26\Pi$, green: $\delta_a \sim 0.976\Pi$, $\delta_c \sim 1.038\Pi$, red: $\delta_a \sim 0.90\Pi$, $\delta_c \sim 0.83\Pi$, respectively). The optical length difference (L) causes the two beams (r_1 and r_2) to be exactly out of

© 2011 WILEY-VCH Verlag GmbH & Co. KGaA, Weinheim

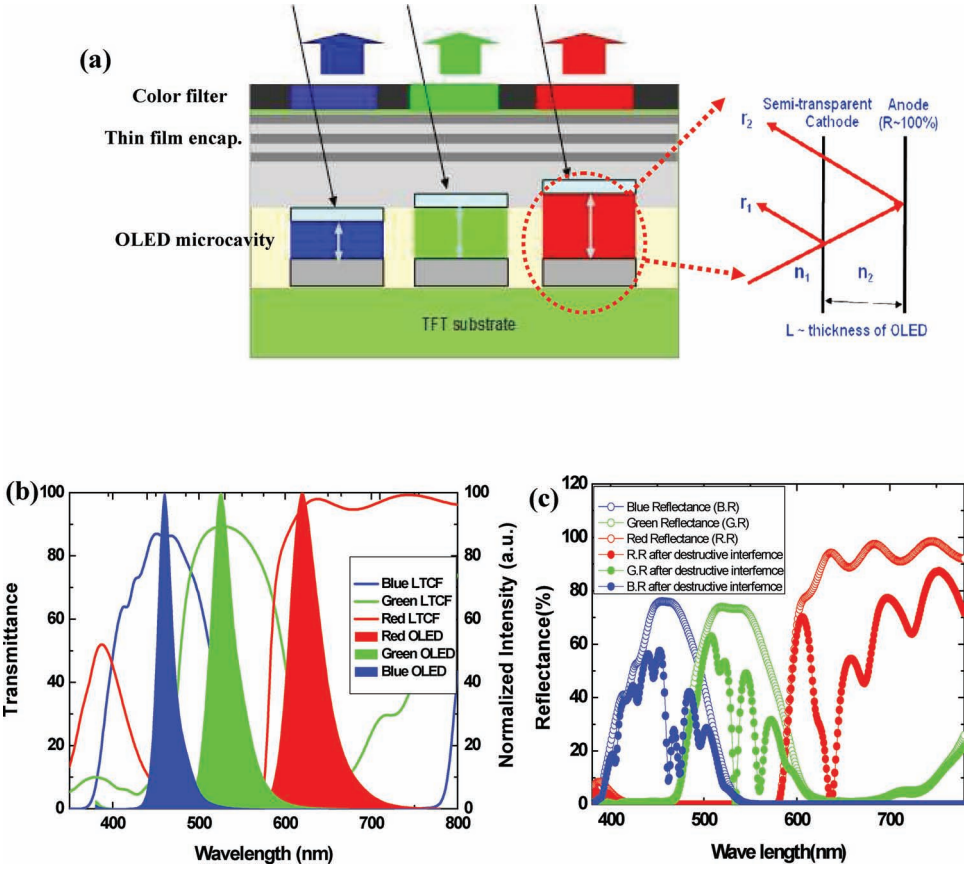

Figure 2. a) Schematic view of a new optical system for a flexible display device composed of a LTCF, TFE, and a RGB OLED microcavity. (inset) The structure of the RGB microcavity: The different thicknesses of the RGB OLED layer are primarily designed to the optical length (L) of the RGB cavity to form a standing wave inside the optical resonator. To undergo fully destructive interference of reflective lights between the semi-transparent cathode and reflective anode, the optical length (L) of the OLED should be equal to an integer multiple of primary color (λ_n). b) Transmittance of the LTCF and typical OLED microcavity EL spectra. The EL peak position of the OLED exactly corresponds to the maximum transmittance of the LTCF. c) The comparison of the measured data for the reflectance produced by only color filters and LTCFs with an OLED microcavity to verify the effect of a destructive interference of the microcavity.

phase, producing fully destructive interference. Furthermore, if sufficient EL light exists in a microcavity, the electromagnetic radiation builds up the microcavity resonance created by the standing wave formed between the mirrors.[12] That is, the top-emission microcavity forms a destructive interference for outdoor light and a constructive interference for the EL light inside the OLED structure. Figure 2b shows the measured normalized EL spectra for the RGB OLED microcavity at the maximum luminescent voltage, where the EL peak positions of the RGB OLED microcavity correspond exactly to the peak transmittances of the RGB color filters. The full width at half maximum (FWHM) of the EL peaks through the optical microcavity (similar to a Fabry–Perot interferometer) are estimated as 21 (blue), 32 (green), and 42 nm (red). Figure 2c shows the measured reflectance produced by unit pixels (RGB color filters with RGB OLED microcavity) to verify the effect of destructive interferences of the microcavity in achieving low overall reflectance. As shown in **Figure 3**a the contrast ratio under a lighted ambient (500 lux) is enhanced using a combination of color filters and OLED microcavity. Based on a WVGA (display resolution: 800 × 480 pixels) OLED panel, a contrast ratio of 14:1 and 150 000:1 is achieved with outdoor lights of 500 lux and dark ambient, respectively. As shown in Figure 3b, a low reflectance of 7.1% through the combination of color filters and microcavity is comparable with that of a conventional POL film (7%) while a dramatic improvement from OLED panels without color filters (60%) is observed.

By using a combination of color filters and an OLED microcavity not only the outdoor readability improves but low power characteristics are achieved as the driving power, compared to conventional OLED technology, is reduced by more than 30%. Current OLED technology utilizes a POL film to improve outdoor readability, but POL films fundamentally attenuate electroluminescent light by about 56% in our experiment. In comparison, the combination of color filters and an OLED microcavity allows electroluminescent light to pass through with a transmission range of 70–95%. A more than 30% of differential transmission through the LTCF compared to POL films helps to reduce the consumption energy by up to 40% when the same output luminescence is achieved. Experimentally, an OLED panel based on POL films should be driven at a power of 768 mW to achieve a brightness of 200 cd m^{-2}.

© 2011 WILEY-VCH Verlag GmbH & Co. KGaA, Weinheim

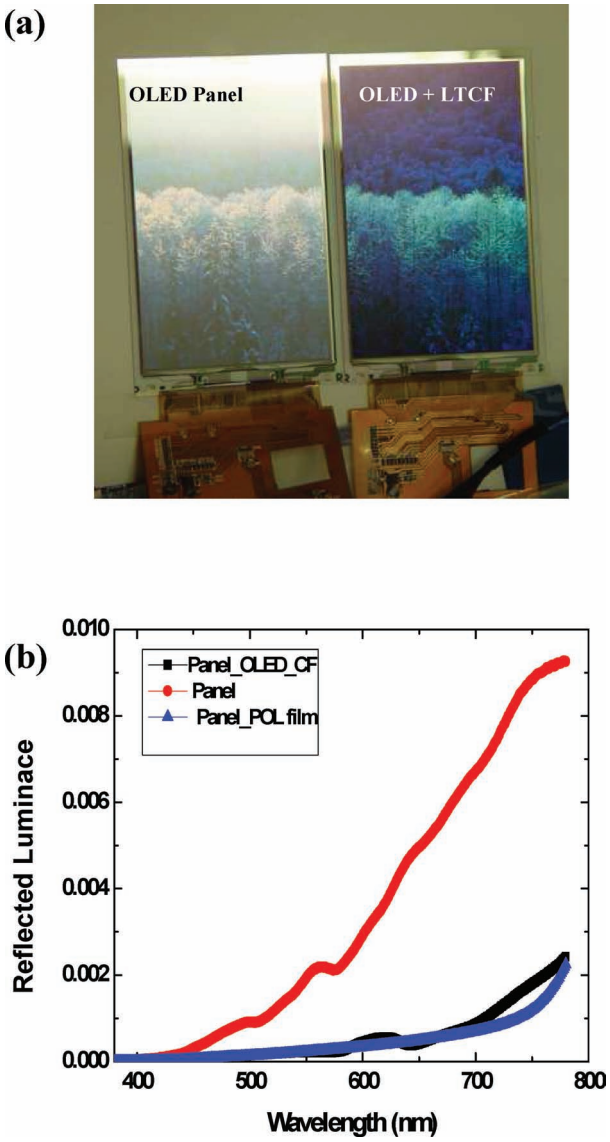

Figure 3. a) Optical image of an OLED panel (left) and an OLED panel with color filter (right). At an ambient light of 500 lux, the left panel shows a poor image, owing to a high reflectance of outdoor light while the right panel has a well-defined and readable image. b) The optical measurements of reflectance at 500 lux are 62% for the OLED panel only, 7.0% for the OLED panel with POL films, and 7.1% for the OLED panel with color filters and microcavity.

A similar panel implemented with an OLED microcavity and color filters is driven at 519 mW to achieve the same brightness, a 34% reduction in power consumption.

Key challenges to fabricate commercial flexible OLEDs is the requirement that all components be compatible with a reliability of the OLED without any damage. As suggested by our novel architecture, a color filter with a microcavity can improve outdoor readability, and the color filter is capable of being bent or twisted. However, standard color filter processing relies upon photoresists that require a hard baking step at temperatures exceeding 200 °C to achieve polymer crosslinking. Such high temperature treatments give rise to damaged OLED devices and deformation in flexible plastic substrates. In order to lower the baking temperature to achieve polymer crosslinking, a LTCF process is specially developed with a photoresist composition (by BASF) based on diacrylate which allows a high crosslinking degree of about 80% with low temperature treatment of 65 °C and UV curing. Instead of a conventional acrylate crosslinking monomer, 1,4-butylene glycol diglycerolate diacrylate is used (see the inset of **Figure 4**a). Figure 4a shows the normalized IR absorption of the double bonding acrylate for photopolymerization by UV light with a wavelength of 400 nm and concurrent heat treatment, where the absorption is observed between 800 and 818 cm^{-1}. The intrinsic absorption (black line) prior to post-treatment corresponds to 0% crosslinking (no light exposure; 100% of double bonds), while 100% crosslinking (red line) corresponds to a UV curing at 3900 mJ followed by a post-baking at 200 °C to force the remaining double bonds to crosslink. LTCFs (blue line) using the selected diacrylate monomers achieve a sufficient crosslinking degree of about 80% through UV curing of 1560 mJ, and the resulting layer can be resistant against subsequent color filter processing (second and third layers) and maintain other advantageous features such as dispersion stability, solubility, and chemical resistance.

In this new scheme for flexible OLED technology, TFE of multi-pairs of an inorganic oxide (Al_2O_3) and polyacrylate are employed to protect the OLED from ambient oxygen and water, as an alternative to glass encapsulation. The inorganic oxide layers function as diffusion barrier against water/oxygen molecules and the polymer layers provide flexibility and oxide defect coverage. The process is performed at temperatures under 80 °C, thus it is compatible with OLED devices and the plastic substrate. The major effect of multilayer encapsulation is to increase the lag time for water molecules and oxygen molecules to reach the OLED devices. The reliability of the TFE is tested by soaking the display in water while monitoring the brightness of the OLED versus the soaking time as shown in Figure 4b. Even after soaking the panel in water for 1 h, no variation in the OLED brightness was observed indicating the implementation of a pinhole-free encapsulating layer that provides a highly reliable OLED panel.

The mechanical folding tolerance test for the flexible OLED display device on a polyimide substrate is performed under tensile stress using a mechanical folding system (**Figure 5**a) and SpectraScan Colorimeter (Photo Research, Inc). The sample for folding experiments includes an OLED, TFE, and LTCF (flexible display device) deposited on a 500 nm thick polyimide film, where the sample does not have the electronic circuitry. The representative flexible OLED display device exhibits an overall thickness of 8 μm, allowing it to be bendable and foldable. Folding experiments are carried out on a window module with a folding radius of 1 mm and measurements are recorded every 1000 folds around the hyperelastic areas as shown in Figure 5b. Seven points of relative brightness compared to the original brightness are measured. The variation of relative brightness is within 6% of the original brightness (below human eye recognition) after folding 10 000 times.

Possible application of the present flexible OLED display devices is as a seamless/foldable display and ultra-thin flexible display as shown in **Figure 6**. A fully flexible OLED

© 2011 WILEY-VCH Verlag GmbH & Co. KGaA, Weinheim

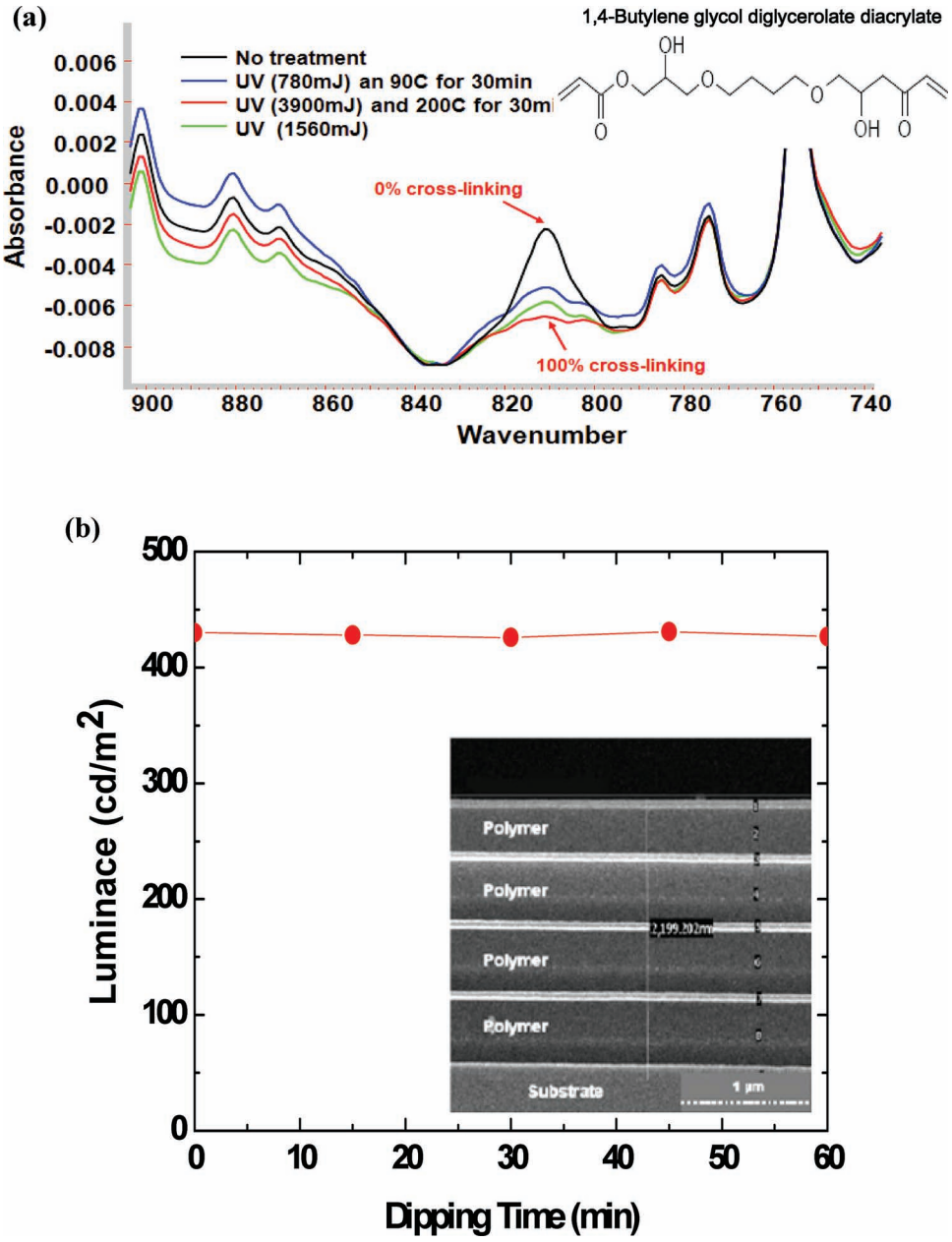

Figure 4. a) IR absorption of double bonding acrylate with various treatments: i) no treatment (black), ii) the proposed recipe (blue), iii) long UV curing (green), iv) long UV curing and post-baking at 200 °C (red). b) Reliability test for OLED brightness as a function of dipping time in water. (Inset) The SEM image of multi-pair organic/inorganic TFE produced with Vitex.

display requires that a flexible backplane that contains driving/switching thin-film transistors (TFTs) and capacitor must be integrated with the flexible display devices suggested here. To minimize the mechanical stress, a flexible backplane has been manufactured with supporting plastic layers, where the neutral plane[13–16] is defined as strain free zones under both inward and outward bending as shown in Figure 6a. Importantly, recent research experimentally reported that TFTs and electrical devices placed on a neutral plane fabricated on a plastic substrate (polyimide) achieved a stable performance under 20 000 times tensile and compressive bending down to radii of 3 mm.[15] Figure 6b shows a possible application of a seamless/foldable OLED display including flexible OLED display devices, composed of two individual OLED panels[17,18] that pretend to display a single unfolded shape, but with a LTPS backplane implemented on a glass substrate with small mechanical flexibility compared to the flexible LTPS backplane.[16] The glass substrate is thinned to 50 μm by chemical mechanical polishing (CMP) and is subsequently integrated with two thick protecting layers (~500 μm) on each side to form a neutral plane. For future flexible display technologies, the development of the present flexible display device incorporating a flexible backplane[16] on a plastic substrate is expected to revolutionize the implementation of flexible displays.

© 2011 WILEY-VCH Verlag GmbH & Co. KGaA, Weinheim

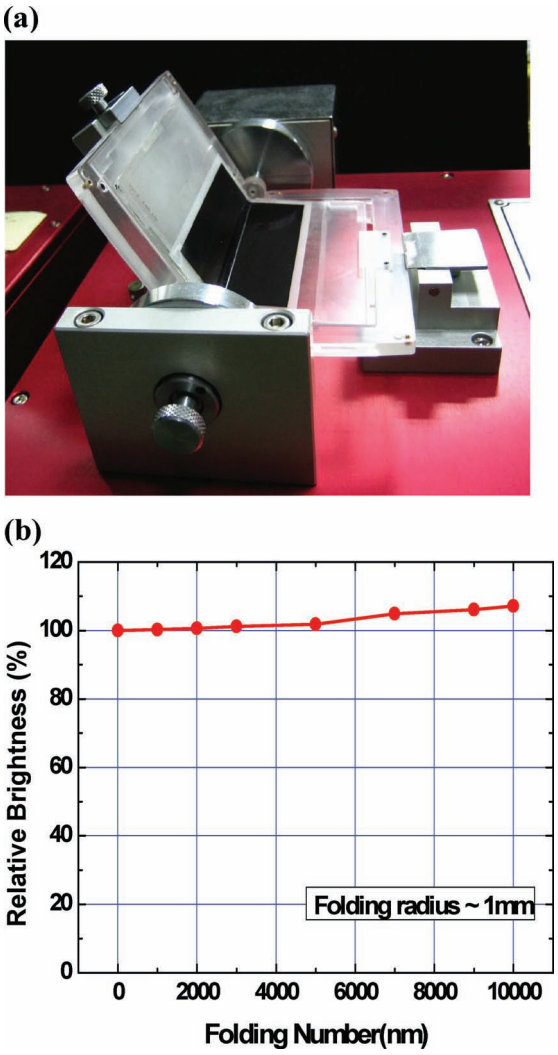

Figure 5. a) Experimental setup for mechanical folding test. b) Optical measurement of a flexible OLED device after folding a 1 mm radius window module. Relative brightness is monitored in steps of 1000 folds for a total 10 000 folds.

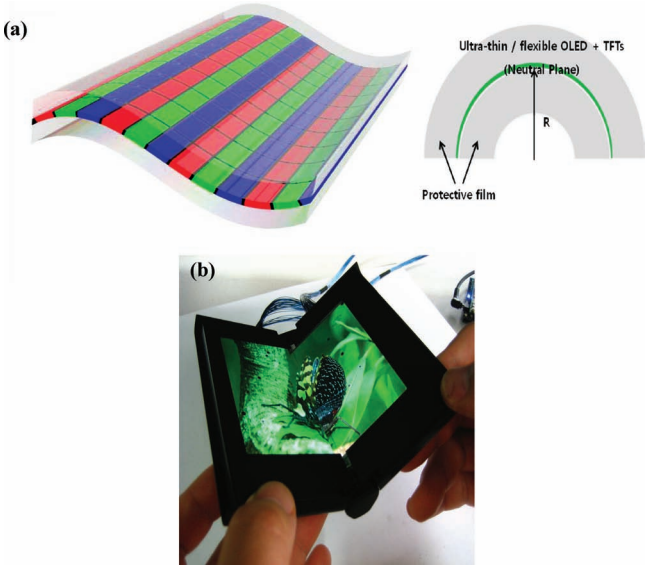

Figure 6. a) A schematic view of a neutral plane used to eliminate strain applied at a backplane and OLED device. b) Foldable/seamless OLED display: a foldable OLED display is fabricated by arranging two OLED panels and one transparent plane. The left OLED panel is slimmed down to 50 μm and assembled on the transparent plane.

Acknowledgements

The authors thank Woo Sung Jeon, Miok Shin, and SeungYeon Lee for their help in measuring the reflectance of the unit pixel, and for in-depth discussion on material properties of color filters. Furthermore, the authors thank G. D. Keyzer (BASF) for his help in the development of a low-temperature color filter.

Received: March 23, 2011
Published online: July 7, 2011

[1] A. Chen, J. Au, A. Kazlas, R. H. Gates, M. McCreary, *Nature* **2003**, *423*, 136.
[2] S. Ju, J. Li, J. Liu, P. Chen, Y. Ha, F. Ishikawa, H. Chang, C. Zhou, A. Facchetti, D. B. Janes, T. J. Marks, *Nano Lett.* **2008**, *8*, 997.
[3] S. Bae, H. Kim, Y. Lee, X. Xu, J. Park, Y. Zheng, J. Balakrishnan, T. Lei, H. R. Kim, Y. I. Song, Y. Kim, K. S. Kim, B. Ozyilmz, J. Ahn, B. H. Hong, S. Iijima *Nat. Nanotechnol.* **2010**, *5*, 574.
[4] K. Nomura, H. Ohta, A. Takagi, T. Kamiya, M. Hirano, H. Hosono, *Nature* **2004**, *432*, 488.
[5] H. Kim, K.-B. Park, K. S. Son, J. S. Park, W.-J Maeng, T. S. Kim, K.-H. Lee, E. S. Kim, J. Lee, J. Suh, J. B. Seon, M. K. Ryu, S. Y. Lee, K. Lee. *S. Im. Appl. Phys. Lett.* **2010**, *97*, 102103.
[6] J. Jang, *Mater. Today* **2006**, *4*, 46.
[7] S. Kim, S. Kim, J. Park, S. Ju, S. Mohammadi, *ACS Nano* **2010**, *4*, 2994.
[8] S. Kim, S. Ju, J. H. Back, P. D. Ye, M. Shim, D. B. Janes, S. Mohammadi, *Adv. Mater.* **2008**, *20*, 1.
[9] D. J. Gundlach, J. E. Royer, S. K. Park, S. Subramanian, O. D. Jurchescu, B. H. Hamadani, A. J. Moad, R. J. Kline, L. C. Teague, O. Kirillov, C. A. Richter, J. G. Kushmerick, L. J. Richter, S. R. Parkin, T. N. Jackson, J. E. Anthony *Nat. Mater.* **2008**, *7*, 216.
[10] L. L. Moro, T. A. Krajewski, N. M. Rutherford, O. Philips, R. J. Visser, *Proc. SPIE.* **2004**, 83, 5214.
[11] T. Todorov, L. Nikolova, N. Tomova, Appl. *Optics* **1984**, *23*, 4309.
[12] G. R. Fowles, *Introduction to Modern Optics* Dover Publication, Inc. **1968**.
[13] D. Jin, J. Jeong, T. Kim, J. Lee, T. Ahn, Y. Mo, H. Chung, *J. Soc. Inf. Display* **2006**, *14*, 1083.
[14] Z. Suo, E. Y. Ma, H. Gleskova, S. Wanger, *Appl. Phys. Lett.* **1999**, *74*, 1177.
[15] H. Gleskova, S. Wagner, Z. Suo, *Appl. Phys. Lett.* **1999**, *74*, 3011.
[16] S. An, J. Lee, Y. Kim, T. Kim, D. Jin, H. Min, H. Chung, S. Kim. *Soc. Inf. Display(SID) Symp. Digest* **2010**, 47, 706.
[17] H. Shim, I. Kee, S. Kim, Y. Chun, H. Kwon, Y. Jin, S. Lee. *Soc. Inf. Display(SID) Symp. Digest* **2010**, 41, 257.
[18] H. Kwon, H. Shim, S. Kim, W. Choi, Y. Chun, I. Kee, S. Lee, *Appl. Phys. Lett.* **2011**, *98*, 151904.

© 2011 WILEY-VCH Verlag GmbH & Co. KGaA, Weinheim